Thermochimica Acta, 119 (1987) 189-201
Elsevier Science Publishers B.V., Amsterdam — Printed in The Netherlands

DECONVOLUTION OF PERIODIC HEAT SIGNALS BY FAST FOURIER TRANSFORM

K.H. Müller and Th. Plesser

Max-Planck-Institut für Ernährungsphysiologie
Rheinlanddamm 201, D-4600 Dortmund 1 (FRG)

SUMMARY

The simultaneous measurement of the rate of heat production and of at least one other physical signal generated by an oscillating chemical or biochemical reaction is a promising tool for the elucidation of the underlying reaction steps and their correlation in time. An essential prerequisite for the interpretation of the experiments is the deconvolution or "desmearing" of the recorded signals. The usefulness of Fast Fourier Transform (FFT) algorithms for the deconvolution is shown by numerical simulations. Various systematic errors superimposed on the "true" signal by the time resolution of the apparatus in use are analyzed as well as statistical noise and serially correlated errors in the measured data. A short description of a robust and easy to use software package of the deconvolution algorithm is given. The package is written in FORTRAN 77 and executable on personal computers and mainframes.

INTRODUCTION

Measurements of time dependent processes in systems of finite size are biased by systematic errors originating from the inevitable inertia of the mass of the system under investigation. These inertia effects are very pronounced in devices for the detection of heat or electrode potentials, since diffusion processes play a crucial role. On the other hand most optical methods, for example the absorption of light, may be considered as instantaneous techniques for monitoring chemical or biochemical processes. The simultaneous measurement of the rate of heat production with a microcalorimeter and of at least one other physical signal of an oscillating chemical or biochemical reaction is a promising tool for the elucidation of the underlying reaction steps and their correlation in time (ref. 1,2). The interpretation of the measured signals, especially the comparison of the shape of the waves and the estimation of phase relations, are not straightforward due to the different time behaviour of the signal detectors resulting in a "smearing" of the "true" signal generated in the sample under investigation. The "smearing" effect must also be taken into account

0040-6031/87/$03.50

for the calculation of the amount of heat having evolved within finite time intervals for instance during one period. Only the total heat produced is time independent and therefore independent of the inertia of the calorimeter.

From these arguments it becomes clear, that the type of experiments under consideration are useful only if the "true" signals can be extracted from the measured data by mathematical "desmearing" or deconvolution techniques (ref. 3).

In the following chapter, the basic mathematical formulas for the deconvolution by Fourier transform are given and the special arrangement of the data for the use of discrete Fast Fourier Transforms (FFTs) is described. A computer program is introduced which performs the whole data analysis. The capabilities and limitations of the deconvolution technique applied to periodic signals are demonstrated in the second half of the paper.

NUMERICAL METHODS

A signal recorded by means of any time dependent physical instrument results from the interplay of at least two sources, the "true" signal produced by the specimen under investigation and its broadening by the measuring device. The most significant impact of the apparatus arises from its inertia to follow the variation of the "true" signal instantaneously. The inertia of a device is quantitatively described by its response to a signal with pulse-like characteristic having a pulse width of the order zero. The response curve r(t) is called the relaxation function, response function, or transfer function of the device.

The functional relation between the "true" and the recorded signal is given by the following integral expression (ref. 4).

$$\varphi(t) = \int_{-\infty}^{+\infty} r(t-t')f(t')dt' \qquad (1)$$

This formula means that the measured signal $\varphi(t)$ is a convolution of the "true" signal f(t) with the response function r(t). In other words, the signal φ at time t is the integral of all events having taken place at times t′ before t and diminished according to the relaxation of r(t). Equation (1) is a correct description of the physics of the measurement, provided that the normalized response function is independent of the amplitude of

the input pulse. An apparatus with this property is called a linear device. In the following, we presuppose that the response function is normalized and in addition it should be noted that by definition $r(t)=0$ for $t \leq 0$ holds.

For a pulse-like response function, $r(t)$ can be approximated by Dirac's delta function. In this case it is found from equation (1) that the recorded signal is identical with the "true" signal.

Sophisticated deconvolution techniques must be applied if the response of the apparatus has significant effect on the physical signal one is interested in. Three numerical approaches have been considered in literature. 1) The "direct" method by matrix inversion, 2) several iterative procedures, and 3) the deconvolution by Fourier transforms. We discuss only the latter one. A discussion about advantages and disadvantages of the various methods may be found in (ref. 5-8).

The deconvolution by Fourier transforms is based on the convolution theorem for an equation as of type (1). This theorem states that the Fourier transform of the convolution integral is given by the product of the Fourier transform of each function (ref. 4,9). The application of this theorem to equation (1) results in (2).

$$\mathcal{F}(\varphi(t)) = \mathcal{F}(r(t)) \cdot \mathcal{F}(f(t)) \tag{2}$$

$\mathcal{F}$ is a short form of the Fourier integral, the transition from the time domain into the frequency domain. Its definition together with the inverse operation is given by following equations

$$\mathcal{F}(\varphi(t)) = \hat{\varphi}(\omega) = \int_{-\infty}^{+\infty} e^{-2\pi i\omega t}\, \varphi(t)\, dt$$

$$\mathcal{F}^{-1}(\hat{\varphi}(\omega)) = \int_{-\infty}^{+\infty} e^{2\pi i\omega t}\, \hat{\varphi}(\omega)\, d\omega \tag{3}$$

The calculation of $f(t)$ is straightforward since with

$$\mathcal{F}(f(t)) = \mathcal{F}(\varphi(t)) / \mathcal{F}(r(t)) \tag{4}$$

the inverse Fourier transform of (4) unveils the true signal

$$f(t) = \mathcal{F}^{-1}\left(\mathcal{F}(\varphi(t))/\mathcal{F}(r(t))\right) \qquad (5)$$

This elegant solution of the deconvolution problem has some drawbacks. The most obvious one is the large computation time for the Fourier transforms. This problem can be minimized by the application of Fast Fourier Transform (FFT) techniques (ref. 9,10, 11). The only prerequisites for the applicability of FFTs are that the data points are equidistant in time and that their number is a power of two. More serious are the implicit properties of Fourier transforms, the amplification of noise and the sensitivity with respect to cut-off errors. Noise reduction may be achieved by smoothing techniques, for example by splines (ref. 11,12) or polynomes (ref. 13); cut-off effects can be reduced by suitable extensions of the measured functions.

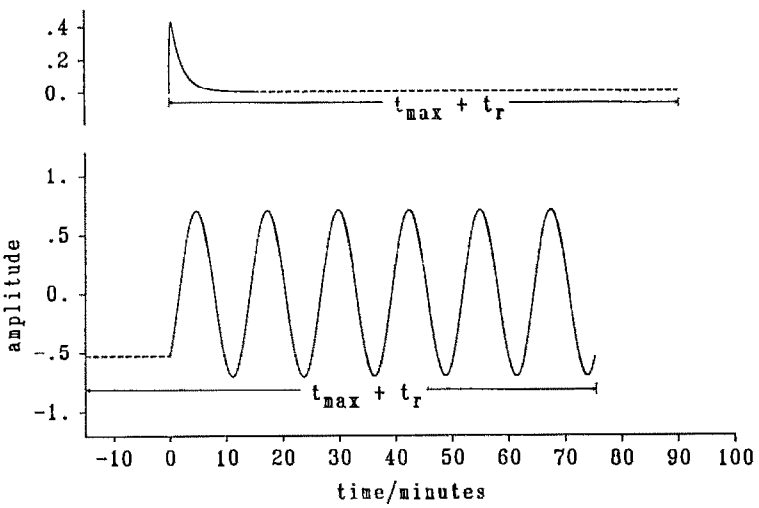

Fig. 1 The measured function $\varphi(t)$ (below) and the response function r(t) (above) are shown by solid lines. The dashed lines display the extensions resulting in an identical time interval for both curves.

The conversion of the outlined mathematical procedure into an easy-to-use and robust numerical software package needs some carefully chosen extensions of the measured data sets for the minimization of cut-off errors.

Assume that $\varphi(t)$ is measured in the interval $0 \leq t \leq t_{max}$ and $r(t)$ in the interval $0 \leq t \leq t_r$. Both functions have to be adapted for FFT to a time interval of identical length $t_{max} + t_r$ as shown in Fig. 1. The resolution function can smoothly be extended beyond t if $r(t)$ has been measured over such a long time interval that $r(t_r) \simeq r(0) \simeq 0$ holds. In this case $r(t) = 0$ is a rational extension for $t > t_r$. Cut-off effects in the deconvoluted data at t=0 can be minimized by extending $\varphi(t)$ into the negative time range at least of length $-t_r$. The only appropriate choice for φ values in this interval is $\varphi(t) = \varphi(0)$ for $-t_r \leq t \leq 0$. The various steps of the whole deconvolution procedure are summarized in the block diagram of Fig. 2.

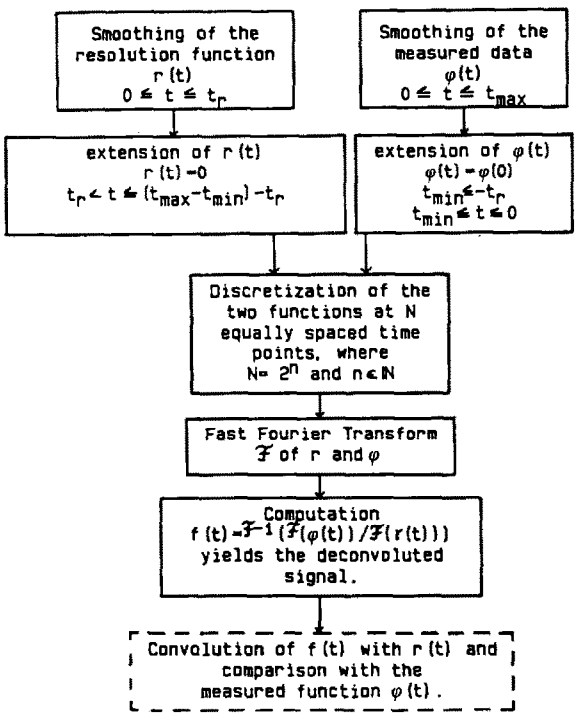

Fig. 2 Block diagram of the processing procedures for data deconvolution by Fast Fourier Transform.

The last step, the convolution of $f(t)$ and $r(t)$ by numerical integration, has been included for a final control of the errors which may have been accumulated during the various numerical procedures. A graphic presentation of the measured data $\varphi(t)$ and

their numerically recalculated counterpart immediately gives an impression of the accuracy of the deconvolution and the precision of the underlying measurements of f(t) as well as of r(t). The procedure shown in Fig. 2 has been transposed into a FORTRAN 77 compatible software package executable on mainframes and on personal computers equipped with a coprocessor for floating point operations. The performance is in the time range of seconds (see table 1 below).

NUMERICAL SIMULATIONS

The capabilities and limitations of the deconvolution procedure explained in the last chapter are favourably demonstrated by functions which can be handled analytically. It is obvious that periodic behaviour is modelled by sine or cosine and the response function of the apparatus by a sum of exponentials as given in (6).

$$r(t) = C \sum_i A_i e^{b_i t} \qquad t > 0 \; ; \quad r(t)=0 \text{ for } t \leq 0 \tag{6}$$

with

$$C = \frac{1}{\sum_{i=1}^{n} \frac{A_i}{b_i}} \tag{7}$$

The constant C follows from the normalization condition . An additional constraint for the amplitudes turns out from the condition $r(t=0) = \sum_{i=1}^{n} A_i = 0$.

The convolution of the response function (6) with a periodic signal with frequency ω $f(t)=\sin(\omega t)$ results in

$$\varphi(t) = \sum_{i=1}^{n} \frac{A_i}{b_i^2+\omega^2} \left(\omega\cos(\omega t) - b_i \sin(\omega t)\right) \tag{8}$$

For the numerical work we have chosen a response function with $n=2$, $b_1=0.5/\text{min}$, and $b_2=10/\text{min}$ for the time constants and $A_1=-1.0/1.9$ $A_2=1.0/1.9$ for the amplitudes, which are uniquely defind for the case $n=2$ when b_1 and b_2 are given. b_1 determines the relaxation of the response curve with a relaxation time $1/b_1=2$ min. The response function with the just given parameters

is referred to as the two-exponential response function in the following.

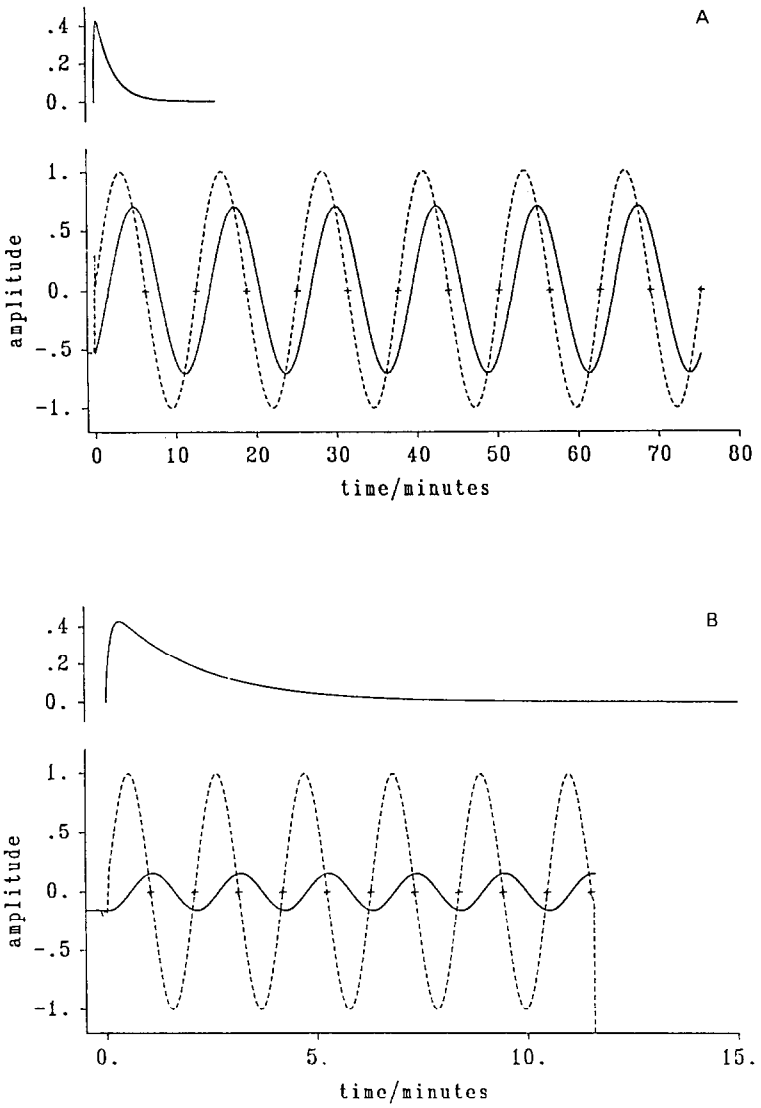

Fig. 3 Numerical deconvolution of the test functions $\varphi(t)$ (solid line in lower parts of the graphs) with the two-exponential response function r(t) (solid line in the upper parts of the graphs). The dashed lines show the expected results: (A) f(t)=sin(0.5 t) and (B) f(t)=sin(3.0 t). Its zeros are marked by (+).

Fig. 3 shows two simulations with ω=0.5/min (Fig. 3A) and ω=3.0/min (Fig. 3B). The periodic solid curves are the "measured" data $\varphi(t)$ simulated with (8) at 750 time points and then fitted by splines (ref. 11) for the selection of 512 data points equidistant in time. The response function in the upper part of the graphs are generated with 300 data points by the same procedure and formula (6). The dashed lines in Fig. 3 represent the functions f(t) after numerical deconvolution using 512 points for the FFTs. The amplitude and the phase are recovered precisely for both frequencies. Since the agreement between the calculated and the assumed functions is so close, the theoretical curves are not drawn in the figures. It should be noted that the deviations at the boundaries of the curves are more pronounced for the higher frequency in Fig. 3B, where the ratio of the time parameters ω/b_1 is 6 compared to 1 in Fig. 3A.

Fig. 4 and 5 summarize the filter properties of the inertia for an apparatus with a given response function, taking the signal frequency ω as the independent variable. The ratio of amplitudes in Fig. 4 is defined as the quotient of the measured and the "true" amplitude. This ratio is less than or equal to 1 by definition. It approaches 1 for very slow processes and zero when the period of the process is close to or even higher than the relaxation time of the response function. The curve marked by squares in the middle of the three lines is calculated with the simulated response function. The other two curves are determined with measured response functions having relaxation times of 2 minutes ($\triangle$) or 2.3 minutes ($\odot$), respectively (see for instance figure 2 in ref. 1). The phase shift subjected to the "true" signal by the time response of the apparatus is given in Fig. 5. In this graph, the data calculated with the simulated two-exponential response curve deviate from the curve calculated with the measured response functions. The different trends of the curves for ω larger than 1/min indicate, that the experimental response curves contain more than one exponential relaxation term for larger times.

All these calculations are performed with error-free data, simulating a by no means realistic situation. The introduction of statistical noise has no significant effect since the noise is almost completely eliminated by the spline fits at the beginning of the data evalution procedure. It is conceivable that independent distortions of the measured data are very unprobable, due to

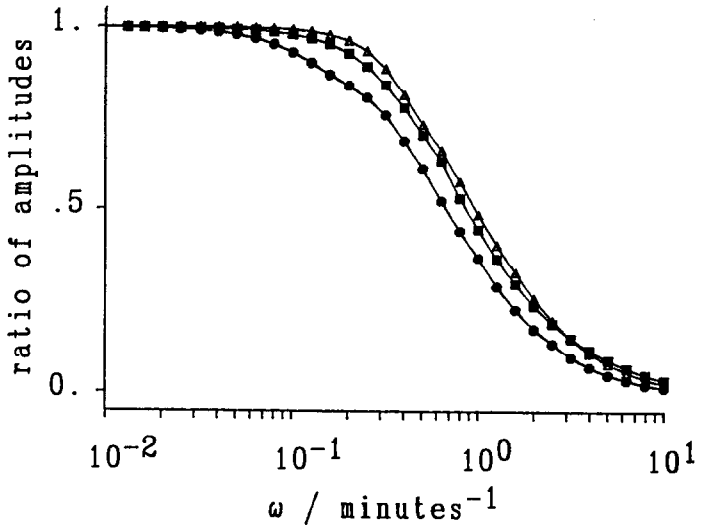

Fig. 4 Ratio of amplitudes as a function of the signal frequency ω. The ratio of amplitudes is the quotient of the amplitudes of the "measured" data $\varphi(t)$ and of the "true" signal f(t). The deconvolution is performed with the two-exponential (⊠) and two experimental response functions (⊙) (△).

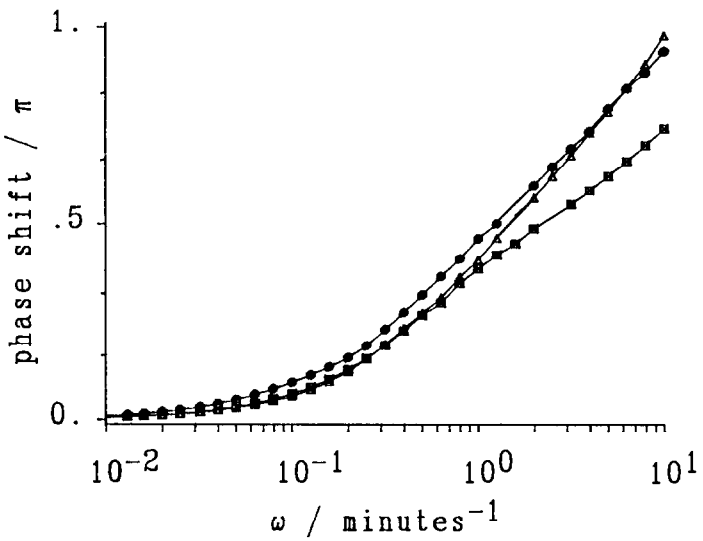

Fig. 5 Phase shift between the "measured" data $\varphi(t)$ and the "true" signal f(t) as a function of the signal frequency ω, calculated for three response functions. The deconvolution is performed with the two-exponential (⊠) and two experimental response functions (⊙) (△).

the inertia of the system. Such systems produce correlated errors, since a pulse-like fluctuation in the experimental sample appears as a long lasting deformation of the recorded data $\varphi(t)$ reflecting the response function.

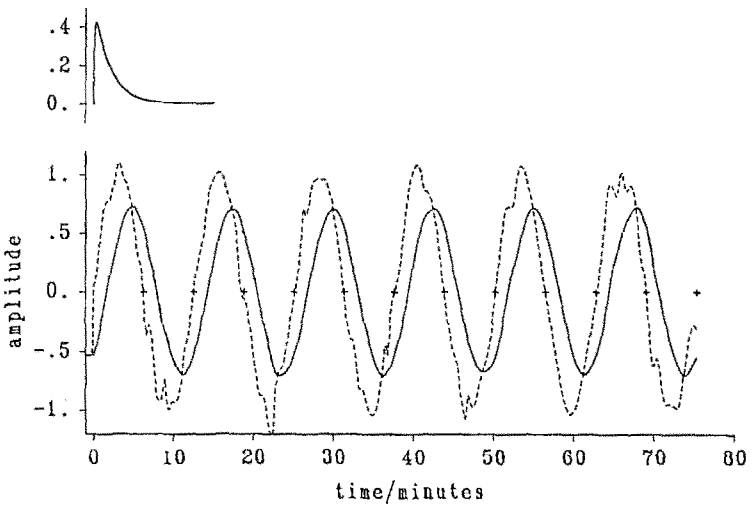

Fig. 6 Numerical deconvolution of the function $\varphi(t)$ superimposed with a correlated error simulated with a standard deviation $\sigma=0.01$ (solid line). The dashed line shows the function $\varphi(t)$ after deconvolution with the two-exponential response curve.

Fig. 6 shows a simulation with $\omega=0.5/min$ and an superimposed error e_j with a strong serial correlation defind at each data point j by

$$e_j = \sum_{i=j}^{j+9} \epsilon_i \qquad (9)$$

ϵ_i is a normally distributed error with standard deviation $\sigma=0.01$. The outcome of the deconvolution with the two-exponential response function is given by the dashed line. The phase shift is recovered as in the error free simulation in Fig. 3A, but the bumps in the dashed curve introduce a great uncertainty in the estimates of amplitudes and even more in the shape of the waves. That serial correlation are significant in real experiments becomes obvious by comparing Figs. 6 and 7. The solid line in Fig. 7 exhibits the periodic heat production accompanied with sugar metabolism in a cytoplasmic medium extracted from yeast (ref. 14,15). The dashed line presents the deconvoluted "true" signal extracted

from the measured data by deconvolution with the experimentally determind response function having a relaxation time of 2.3 minutes. The curve shows bumps similar to the corresponding curve in Fig. 6.

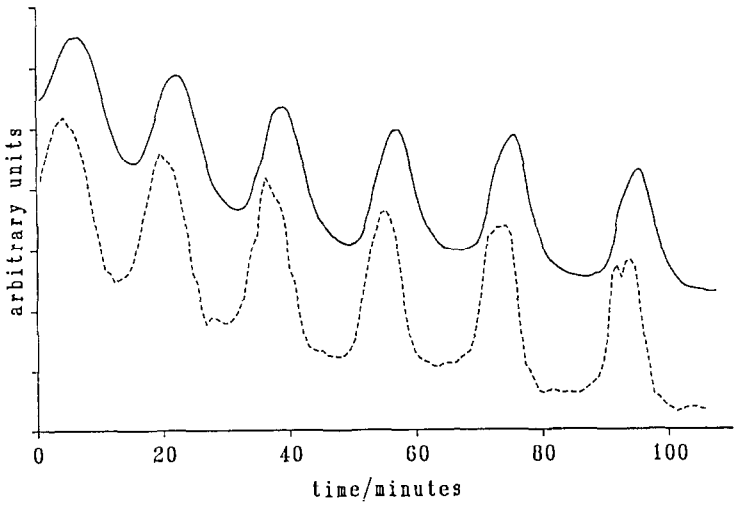

Fig. 7 Rate of heat production measured on a periodically metabolizing cytoplasmic extract from yeast (solid line) and the corresponding deconvoluted signal (dashed line).

Correlated errors are very crucial for the determination of the response function. A good estimate of this function may be found from the average of a set of identical experiments with a pulse-like reaction.

The numerical simulations have been executed on a PERKIN-ELMER 3230 minicomputer. The time required for the whole computation cycle shown in Fig. 2 adds up from the following contributions : 1) time for the spline fits, 2) time for the FFTs and the complex division, and 3) time for the convolution.

For each data set, the spline fit was calculated only once and then stored on disk for later use. The computation of a fit for a typical data set with 700 data points took 30 seconds. Computing times for the FFTs and the convolution are listed in table 1 as a function of N, the number of points used. The computing time increases with order N log(N) for FFT and with order N^2 for the convolution.

TABLE 1
Computation times for the calculation of Fast Fourier Transforms and convolutions as a function of data points N. The time is given in seconds.

N	FFTs	convolution
1024	3.7	38.2
512	1.7	9.6
256	0.8	2.5
128	0.34	0.63
64	0.16	0.17

On a personal computer the time figures have to be multiplied by a factor of about 10.

CONCLUSIONS

In this paper we have outlined the capabilities and limitations of a deconvolution procedure for experimental data recorded as a time series of a periodically evolving process. Careful deconvolution procedures are an essential prerequisite for the correct interpretation of calorimetric experiments undertaken for the elucidation of reaction mechanisms exhibiting a periodic behaviour. The whole procedure for the extraction of the "true" signal from the measured data is assembled in a robust and easy-to-use software package. This fact should lead to a standard procedure for systematic investigations of periodic reactions, as for example the Belousov-Zhabotinskii reaction (ref. 16) or the glycolytic pathway (ref. 14,15). The latter one seems especially promising, since it contains well known reactions steps catalyzed by enzymes. The reaction enthalpies of the steps are known or at least good estimates are available in the literature (ref. 17,18). Another simplifying circumstance is the fact that the enthalpies of the most endothermic step, the splitting of fructose bisphosphate, and of the most exothermic step, the conversion of acetaldehyde into ethanol and CO_2, are by an oder of magnitude larger than the other steps.

The unique advantage of the combination of calorimetry with other continously measurable indicators of a reaction lies in the fact that the rate of heat production gives a quantitative measure of the chemical turnover, i.e. the flux through the system.

ACKNOWLEDGEMENT

We thank Mrs. R. Hübner for skilled assistance during the preparation of the paper.

REFERENCES

1 I. Lamprecht, B. Schaarschmidt, and Th. Plesser, Extended batch calorimetry on periodic chemical reactions, Thermochim. Acta this volume (1987)
2 I. Lamprecht, B. Schaarschmidt, and Th. Plesser, Heat production in oscillating chemical reactions: Three examples, Thermochim. Acta 112 (1987) 95-100
3 W. Hemminger and G. Höhne, Calorimetry, Fundamentals and practice, Verlag Chemie, Weinheim 1984
4 R. Bracewell, The Fourier transform and its application, McGraw Hill,New York, 1965
5 A.F. Carley, R.W. Joyner, The application of deconvolution methods in electron spectroscopy - A Review, J. Electron. Spectrosc. Relat. Phenom. 16 (1979) 1-23
6 E. Cesari, V. Tora, J.L. Maqueron, R. Probst, J.P. Dubes, H. Tachoire, Thermogenese: Application des filtrages electrique et numerique inverse en calorimeter a conduction, Thermochim. Acta 53 (1982) 1-15
7 E. Cesari, V. Tora, J.L. Maqueron, R. Probst, J.P. Dubes, H. Tachoire, Thermogenese: Application comperative de l'analyse harmonique et du filtrage inverse, Thermochim. Acta 53 (1982) 17-27
8 E. Cesari, J. Vinals, V. Torra, J. Ortin, J.L. Maqueron, J.P. Dubles, H. Tachoire, Microcalorimetrie et Thermogenese: Identification des dispositifs experimentaux permettant de mesurer directement les enthalpies d'exces, Thermochim. Acta 79 (1984) 23-24
9 D.F. Elliot, K.R. Rao, Fast transforms, algorithms, analysis, applications, Academic Press, New York, 1982
10 J.W. Cooly and J.W. Tukey, An algorithm for the machine calculation of complex Fourier series, Math. Computation 19 (1965) 297-301
11 Harwell Subroutine Library, AERE Harwell, Didcot Oxfordshire, England, 1985
12 C. de Boor, A practical guide to splines, Applied Sciences Vol. 27 Springer, Berlin Heidelberg, 1978
13 A. Savitzky and M.J. Golay, Smoothing and differentiation of data by simplified least squares procedures, Anal. Chem. 36 (1964) 1627-1639
14 Th. Plesser, S.C. Müller, B. Hess, I. Lamprecht, and B. Schaarschmidt, Periodic heat production by oscillating glycolysis in a cytoplasmic medium extracted from yeast, FEBS Lett. 189 (1985) 42-44
15 B. Hess and A. Boiteux, Oscillatory phenomena in biochemistry, Ann. Rev. Biochem. 40 (1972) 237-258
16 R.J. Field and M. Burger (EDs.), Oscillations and traveling waves in chemical systems, Wiley, New York, 1985
17 S. Minakami and C.H. De Verdier, Calorimetric study on human erythrocyte glycolysis. Heat production in various metabolic conditions, Eur. J. Biochem. 65 (1976) 451-460
18 K. Burton, The enthalpy change for the reduction of nicotinamide-adenine dinucleotide, Biochem. J. 143 (1974) 365-368